

Research article

PV-Li-ion-micropump membrane systems for portable personal desalination

Mark P. McHenry^{1,*}, **P. V. Brady**², and **M. M. Hightower**³

¹ School of Engineering and Information Technology, Murdoch University, Australia

² Geoscience Research & Applications Group, Sandia National Laboratories, USA

³ Energy Systems Analysis Department, Sandia National Laboratories, USA

* **Correspondence:** Email: mpmchenry@gmail.com.

Abstract: This research presents a technical simulation of theoretically portable desalination systems utilising low-energy and lightweight components that are either commercially available or currently in development. The commercially available components are small-scale flexible and portable photovoltaic (PV) modules, Li-ion battery-converter units, and high pressure low voltage brushless DC motor-powered micropumps. The theoretical and conventional small-scale desalination membranes are compared against each other: low-pressure reverse osmosis (RO), nanofilters, graphene, graphene oxide, and graphyne technology. The systems were designed with the identical PV-Li-ion specifications and simulation data to quantify the energy available to power the theoretical energy demand for desalinating a saline water at 30,000–40,000 ppm total dissolved solid (TDS) to reliably supply the minimum target of 3.5 L d⁻¹ of freshwater for one theoretical year. The results demonstrate that modern portable commercially available PV-battery systems and new generations of energy-efficient membranes under development have the potential to enable users to sustainably procure daily drinking water needs from saline/contaminated water resources, with the system exhibiting a net reduction in weight than carrying water itself.

Keywords: desalination; portable; photovoltaic; membrane; graphene

1. Introduction

Twenty five percent of the global population live in arid or semi-arid regions, and lack access to quality and reliable water supplies [1]. In addition to basic survival, the provision of quality water avoids many health issues, including digestive tract problems, and quality water is especially important for young children and pregnant women [2]. Carrying or transporting water is energy and labour intensive and expensive, and is susceptible to supply interruption [1,3]. Similarly, diesel fuel and associated transport costs can be very high in many remote areas, and utilising renewable energy desalination systems is a promising opportunity [3]. Water-limited regions often have excellent solar resources, and small-scale photovoltaic (PV) systems coupled to suitable water treatment technologies are increasingly able to cost-effectively supply this demand [4,5]. Traditional direct solar thermal-powered desalination remains an attractive option for small-scale desalting in remote regions with several competitive advantages, including very low operating costs, no moving parts, and low operational maintenance [2,6,7]. However, traditional solar desalination/distillation systems exhibit low productivity ($3\text{--}4 \text{ L d}^{-1} \text{ m}^{-2}$), medium efficiency ($\sim 35\%$) and are generally large stationary systems [6,7]. In practice many traditional solar desalination/distillation facilities are abandoned due to basic operational issues, or the availability of alternative water sources [7].

The objectives of this research are to overcome water transport challenges for individuals, the low utility of traditional solar desalination/distillation systems and impracticalities of larger systems for personal use, and the intermittency of solar energy resources with selected desalination technologies under development. This research focuses on using portable light-weight PV-based systems to supply sufficient drinking water suitable for remote individuals, without using conventional heavy lead-acid battery energy storage by utilising Li-ion batteries and high-efficiency micropumps. A portable desalination unit is a suitable option to remove water contaminants and treating the very high salinity groundwater (up to 30,000–40,000 ppm TDS, primarily NaCl) for supplementing dwindling drinking water supplies. This research includes simulated technical outputs of the PV-Li-ion-micropump-membrane system, based on known manufacturer and performance data of commercial systems, and combined with published peer-reviewed efficiencies for prototype low pressure membranes. This research aims to present a potential means for practical desalination systems that provide drinking water from high TDS ground and surfacewaters (salt lakes, creeks, the ocean, etc.), with a strong focus on efficiency and portability. The following criteria were used in the system design:

- Utilise only small-scale PV systems to provide a diesel-independent and portable system suitable to carry on the person with a major focus on system weight and size minimisation.
- Production of a minimum of 3.5 L day^{-1} for the portable system to supply individual drinking water consumption from various high TDS water supplies common to remote regions, including unprotected and seasonal ground and surface waters.
- Efficiency of design to consume the minimum amount of energy per unit of water possible.

2. Selected Remote Solar PV-RO System Characteristics

Solar PV is a promising alternative energy choice for small-scale desalination, particularly in remote off-grid areas with high energy and water service provision costs [9]. A relatively small-scale research hybrid ultrafiltration/RO membrane filtration system located in remote and arid Coober Pedy

in South Australia powered by a PV system (with a single axis east-west tracker) produced 764 L day^{-1} , with a specific electricity consumption of 3.2 kWh m^{-3} [10]. The system was designed to assess (on a small-scale) the ability to cost-effectively replace some of the diesel demand for the existing RO system that supplies the town which consumed around $1,350 \text{ kWh day}^{-1}$. While the system would perform effectively, it was deemed to be impractically expensive at the time for a large town such as Coober Pedy (pop.~3,000) and would require a large PV system area of $1,900 \text{ m}^2$ ($150 \text{ W}_p \text{ m}^{-2}$) of untracked modules [10]. While these systems are clearly inappropriate for portable systems, the fundamental approach remains an attractive option for smaller remote community applications.

Remote area water treatment research in Saudi Arabia by Banat et al. [11] used a 4-stage pre-treatment system to reduce scaling and fouling by incorporating a water softener for preventing scaling enabling higher recovery rates, a $5 \mu\text{m}$ sediment pre-filter, a granular activated carbon filter, and a $1 \mu\text{m}$ filter to pre-treat $1,700 \text{ mg L}^{-1}$ brackish water using a spiral wound OSMONICS TFM-100 RO membrane modules. The water treatment systems was powered by a nominal 433 W_p PV array coupled to a charge regulator and two series connected $12 \text{ V } 230 \text{ Ah}$ lead acid batteries for a 24 V bank to power two high-pressure pumps and ancillary intake and softening pumps with a total load of 830 W_p and an expected 8 hour operation energy demand of around $6,640 \text{ Wh}$ inclusive of losses. The research showed the system was able to produce an average of 40 L h^{-1} from a flow feed of 99 L h^{-1} , with a 34% permeate recovery at 0.45 MPa , with a salt rejection rate of between 97.5–98%, delivering an average specific energy consumption of 26 kWh m^{-3} . This system exhibited a relatively linear relationship with the recovery rates between (30–40% recovery consuming between $19.4\text{--}32 \text{ kWh m}^{-3}$) [11]. While the water output and the PV array are in the order of magnitude for a portable system, it remains a very large and heavy unit. To reduce the burden of battery banks, research by Soric et al. [9] successfully demonstrated a small-scale PV-powered RO desalination unit (a Newport 700 MKII $1 \text{ m}^3 \text{ d}^{-1}$, manufactured by Spectra WaterMaker, USA) designed to use sea or brackish water in a stand-alone power supply system with the use of supercapacitors. The desalination unit incorporated several filters (activated carbon for flush water, a sequential prefilter, and a $20 \mu\text{m}$ and $10 \mu\text{m}$ microfilters, and a high-pressure pump (“Clark pump”) to maintain high pressures ($\sim 700 \text{ psi}$, or $\sim 5 \text{ MPa}$) with pressure recouped from the retentate, coupled to two RO membrane units (Filmtec SW30-2540, each with a surface area of 2.8 m^2 , and a stabilised saltwater rejection of 99.4%). The PV system was a 1 kW array (five PhotWatt PW2050 polycrystalline modules at a nominal 18 V each with four bypass diodes at $\sim 8 \text{ I}_{\text{SC}}$, and $\sim 32.7 \text{ V}_{\text{SC}}$), connected to a regulator and a single 250 F supercapacitor with a maximum voltage of 32 V maintained between 27.8 V and 26.7 V by dumping the PV current at the higher supercapacitor voltage and charging at the lower voltage. The supercapacitor voltage dropped to 26 V when the motor (a nominal $24 \pm 2.4 \text{ V}$) to run the pump started, with the system control disconnecting power to the motor if the supercapacitor was 23.1 V , with the 250 F supercapacitor successfully storing around 40 seconds of pumping power operating between $23\text{--}27 \text{ V}$ providing between $300\text{--}600 \text{ W}$ pump load [9]. This demonstrated the utility of the supercapacitor for short-term storage displacing some of the ability of the lead acid bank, even when a small amount of autonomy is achieved. In practice a larger energy storage capacity for autonomous operation for at least one hour enables a reasonable PV capacity factor, and generally discounts the use of supercapacitors in favour of batteries. Nonetheless, the potential of supercapacitor-based approaches for desalination technologies such as electrodialysis has been demonstrated to be suitable for some lower salt concentration brackish water ($1,000\text{--}3,000 \text{ ppm TDS}$). However, electrodialysis research using even brackish feedwater in

remote central Australia found practical problems due to the fouling of the ion-exchange membranes from build-up of contaminants, particulates, and organic matter that reduce ion flux [12].

2.1. Water system considerations

There is a need for small-scale hand portable water purification systems with the capability to remove suspended solids, high rates of dissolved salts, and microorganisms, that enable individuals to utilise the full range of water resources available in remote areas [13]. Power system constraints of small-scale portable systems and the electricity load profile requires system optimisation and high-efficiency components, with the subsequent selection of the most appropriate desalination technology dependent on a range of factors, including water demand, feedwater salinity, availability of servicing contractors, existing infrastructure, and the user needs and preferences [6]. To date, the numerous small-scale PV-RO systems have been designed and constructed are insufficiently small to provide this niche in high-saline portable water treatment applications. Existing small-scale electrified water purification and desalination systems are large, heavy (particularly the lead acid battery banks), complex, and produce greater than 20 L per day of water, requiring large containers and means to carry the system and the water [13]. This research seeks to present technical simulations where small-scale portable PV-Li-ion battery-micropump desalination systems have the potential to ensure a virtually unlimited supply of personal drinking water at a lower weight than actually carrying water when a saline source of water is available for desalination and bottling. The key element is the continued improvement of high-efficiency RO membranes under development.

Avoiding the frequent and rapid charge and discharge cycles conventional battery systems endure when coupled to renewable energy systems with rapid power fluctuations requires the inclusion of appropriately sized storage technologies with an autonomy of hours with an efficient and simple design [14]. For example, typical stand-alone power supply system motor starting currents can be six-times that of the actual operating current, and the system battery banks commonly endure high burst current discharges from cathodic protection systems and motor starts [15]. In general, battery storage systems in stand-alone power supply systems are less reliable than most other components, and are generally oversized relative to the daily load due to the attempt to maximise battery lifespan to minimise replacement costs [16,17]. Moderating PV fluctuations by utilising appropriate storage technology also offers an additional means to access and store more PV module output. Simple system designs using self-regulating approaches for hybrid motor and storage system charging can be achieved by ensuring the PV module V_{OC} is lower than the voltage needed to overpower/charge a motor/storage technology, yet still sufficient to provide load/charge, respectively [18]. Small PV modules coupled to a suitably sized small DC load (variable speed drives, lighting technologies, power electronics, batteries, supercapacitors, etc.) are a simple PV system design, with motors running faster with increasing PV output [18,19]. However, the defining characteristic of rapid variability of PV systems increases the wear and tear on some equipment, including damaging brushless motors by activating the lock function, or damaging the coil on brush type motors. This research proposes the simplest means to decrease complexity of PV-battery-desalination power systems is to use low voltage/wattage PV systems and a relatively high-capacity lightweight storage technology with high-efficiency micropumps that use smaller brushless DC motors drawing minimal current that generate sufficient flow rates and pressures to operate the RO membranes.

2.2. Energy demand and chemical requirements of existing desalination systems

The thermodynamically minimum energy required to desalinate seawater (assuming 33 g NaCl L⁻¹ at 25 °C) is 0.772 kWh per m³. The most efficient commercial RO technology to date can produce 1 m³ of freshwater from seawater from around 2 kWh of electricity [20]. RO is at present the most common and energy-efficient and cost-effective desalination method for water from around 50,000 ppm TDS and below, using pressure to force freshwater through a semi-permeable membrane that prevents passing of dissolved salts [5,21]. RO comprises half the world's installed desalination capacity due to its decreasing cost and energy consumption, yet still exhibits relatively low flux and requires considerable pre-treatment to ensure fouling is minimised [20,22]. Increased membrane permeability improves the energy efficiency of desalination markedly and reduces membrane area, leading to smaller replacement and maintenance costs [20]. At present RO membranes can produce around 0.01–0.05 L cm⁻² day⁻¹ MPa⁻¹ [20,22] removing monovalent salts and dissolved contaminants, although existing RO membrane pre-treatment is crucial as membranes are sensitive to fouling [5,23]. Improving the robustness, chemical tolerance, and cost-effectiveness of desalination membranes is a major research focus alongside energy efficiency, increasing membrane porosity, and reducing water flux turbulence [2,24–26]. Chlorine tolerant desalination membranes have a major advantage in reducing membrane replacement, backwashing chemicals, and energy efficiency to overcome the increased osmotic pressures due to biofouling [20]. Yet, the current range of commercial RO membranes are polymeric membranes [13,20], which are generally intolerant of chlorine and other disinfectants, and post-treatment water disinfection and mineral reintroduction is sometimes required depending on the system and application [5]. Due to chemical intolerance, lower recovery rates (<20%) are commonly used to reduce issues with scaling and fouling [11], and recovery rates influence energy efficiency, with the recirculation of high-pressure brine streams an important optimisation consideration when recovering energy for high-efficiency operation [5]. Therefore, the improved energy efficiency, reliability, and cost reduction of water treatment for remote areas requires major developments in alternative membrane technologies [2].

3. New Membranes and Graphene-Based Developments

There are a number of promising options for improving RO membrane performance, stability, chemical tolerance, mechanical capacity, and salt rejection, including polymer, zeolite, carbon nanotube, graphene-based technologies. Membranes with imbedded and functionalised 0.8 nm carbon nanotubes through the polymeric barrier have a promising salt rejection of 97.7% and a flux rate of 0.044 L cm⁻² d⁻¹ MPa⁻¹ [20]. Yet, at this time carbon nanotube manufacturing remains expensive and complex, with appropriate diameters suitable for desalination commonly too large using current manufacturing techniques [20,27]. Zeolite membrane development has progressed rapidly in the last decade, yet still remain a very high cost option, and yield lower flux per unit area than the state of the art polymeric RO membranes that comprise the majority of RO installed capacity [13,20]. In general zeolite membrane flux is low due to complex pore architecture [27], and fabrication of thin RO membranes of zeolite is a major challenge to technology scale up [22]. There is also an increasing interest in using compact systems of multi-layered water membranes that are able to mechanically support each other from coarse large solid pre-filters, to porous ceramic

microfilters, and single atom thick membranes, which takes into consideration water treatment needs and mechanical expansion coefficients due to thermal and solution exposure [13].

Atom-thick graphene and related materials such as graphene nanoribbons, graphene oxide, graphane, fluorographene, graphyne, graphdiyne, and porous graphene, are under intense investigation regarding thermal, electronic, photocatalytic, reinforced composite, chemical stability, and conductivity applications and properties [28]. Graphene membranes enable a wider range of pressure, chemical and mechanical operating conditions than RO membrane technologies were historically unable to tolerate [29,30]. When graphite is oxidised the thickness between graphene sheets in the now graphene oxide become nanometre scales, and tend to become folded from their previously flat nature [31]. Graphene oxide (GO) membranes exhibit impressive water flux relative to RO membranes, although at present exhibit poor salt rejection rates of between 10–70%, depending on pH, the salt, and the pressures applied [31,32]. Pure graphene's ability to support sub-nanometre pores due to its high mechanical strength, and its atomic thickness (0.335 nm) has the potential to overcome many manufacturing challenges of larger membranes [13,22]. However, producing monolayer graphene sheets one atom thick with suitable nanoscale pores is a major technical challenge [27], yet the “graphene family” has advanced quickly towards large-scale manufacturability with large sheets available to date [29].

Modelling calculations by Cohen-Tanugi and Grossman [29,30] suggest water flux across a perfect graphene membrane of $10\text{--}100\text{ L cm}^{-2}\text{ day}^{-1}\text{ MPa}^{-1}$ is possible, and with near 100% salt rejection. They found that pore configurations of hydrogenated and hydroxylated pores with water permeability allowing passage of between $39\text{ and }66\text{ L cm}^{-2}\text{ day}^{-1}\text{ MPa}^{-1}$, respectively, at 25°C using water with highly saline concentrations of 72 g L^{-1} . The research determined that in contrast to conventional RO membranes, salt rejection of graphene membranes decreased with higher pressures. Furthermore, new graphene derivatives with properties superior to graphene can be realised through either chemical synthesis or structural functionalisations [28,33]. Depending on the material structure of the “graphene family”, they can be functionalised by chemical addition, which can negatively impact the sought abilities of the original material by disrupting the molecular surfaces that determine its unique properties [34]. Graphyne is also a sub-family of planar sheets one atom wide [27]. The mechanical strength of graphene and graphyne are comparable despite graphyne exhibiting one-third the density of graphene, yet differ with respect to graphyne's non-linear fracture strain and stress dependent on the applied direction and the alignment with carbon triple bonds [33]. Similarly, graphdiyne and graphyne exhibit mechanical strength, high thermal resistance, and have applications as membranes in aqueous solutions with a greater suitability to chemical tailoring than graphene [28,33,34]. Graphyne has yet to be produced in significant quantities [27,28], although molecular dynamics simulation research on pore size effects by Zhu et al. [27] found that γ -graphyne-4 may enable even higher water permeability and salt rejection rates than graphene. The γ -graphyne-4 research by Zhu et al. [27] with four acetylene bonds between two adjacent phenyl rings achieved 100% salt rejection and an unprecedented water permeability of $\sim 13\text{ L cm}^{-2}\text{ d}^{-1}\text{ MPa}^{-1}$, and in contrast to graphene, graphyne desalination efficiency improves with greater pressure, enabling high speed and high efficiency desalination [27]. Graphyne derivatives with a primarily trigonal planar geometry can be functionalised through chemical substitution rather than addition, preserving the physical and electrical properties of the graphene and graphyne, although with enhanced chemical properties [34]. γ -graphyne introduces a triangular pore as it is built on phenyl rings connected to a variable number of acetylene bonds that enable pore size customisation with

water passing through graphyne membranes with pore sizes of no less than three acetylene bonds with significant salt rejection possible with less than five acetylene bonds [27]. While the open edges of a graphyne membrane are not chemically stable, they are able to be terminated covalently with hydrogen atoms [33]. A growing number of graphene-based structures are expected to be synthesised in the near future due to the intensive global interest in carbon-conjugated network structures [27].

4. Materials and Methods

4.1. Meteorological data and assumptions

Ten years of primary climatic (daily, and monthly mean) data were derived from the Bureau of Meteorology (BOM) ground-station at Forrest, WA (Station 011052, Lat.(S): 30.8, Long.(E): 128.1 located 160 m above sea level). The Forrest station was selected for a long-term data set representative of a very remote and arid region near the centre of Australia. RETScreen (version 4) meteorological database transformed the data from the BOM Forrest station [35], and was imported into HOMER version 2.68 beta technical simulation software. HOMER simulated the performance of the PV-Li-ion-micropump system over 10 minute intervals over a one year period. HOMER calculated energy balance calculations of the individual electricity flows to and from each component of the designed system incorporating climatic and load inputs. No assessment of the meteorological data or simulation software was undertaken, as HOMER and RETScreen models have been extensively validated, and BOM has excellent data quality procedures. The annual average solar resource is $5.29 \text{ kWh m}^{-2} \text{ day}^{-1}$, with average ambient temperatures of $17.7 \text{ }^\circ\text{C}$. (Figures 1 and 2).

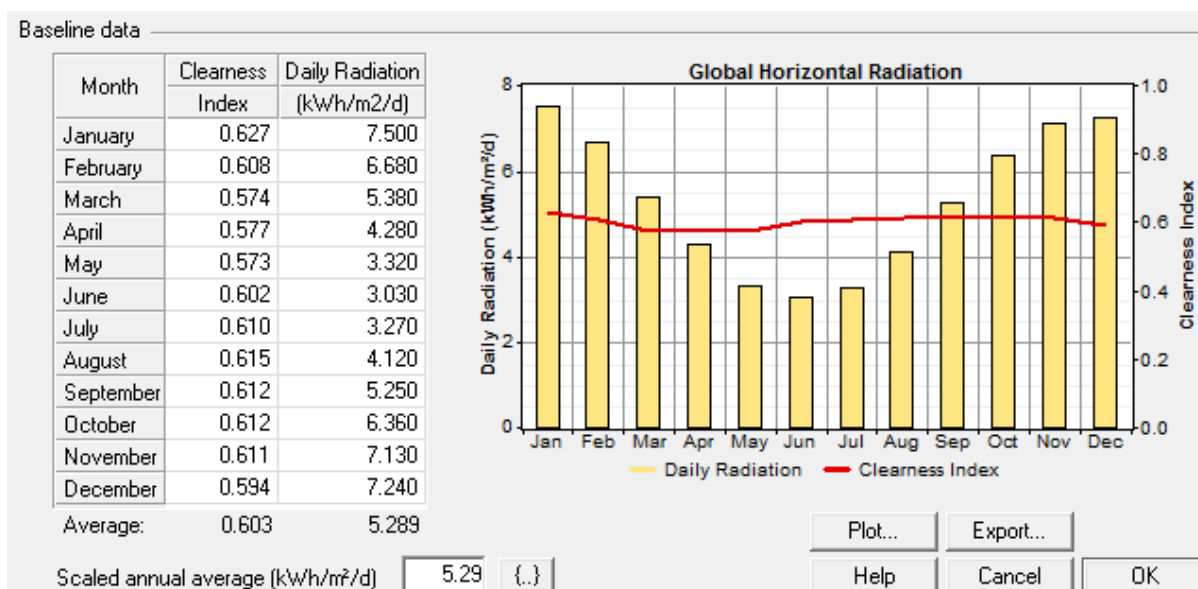


Figure 1. Average monthly daily solar resource at the Forrest station.

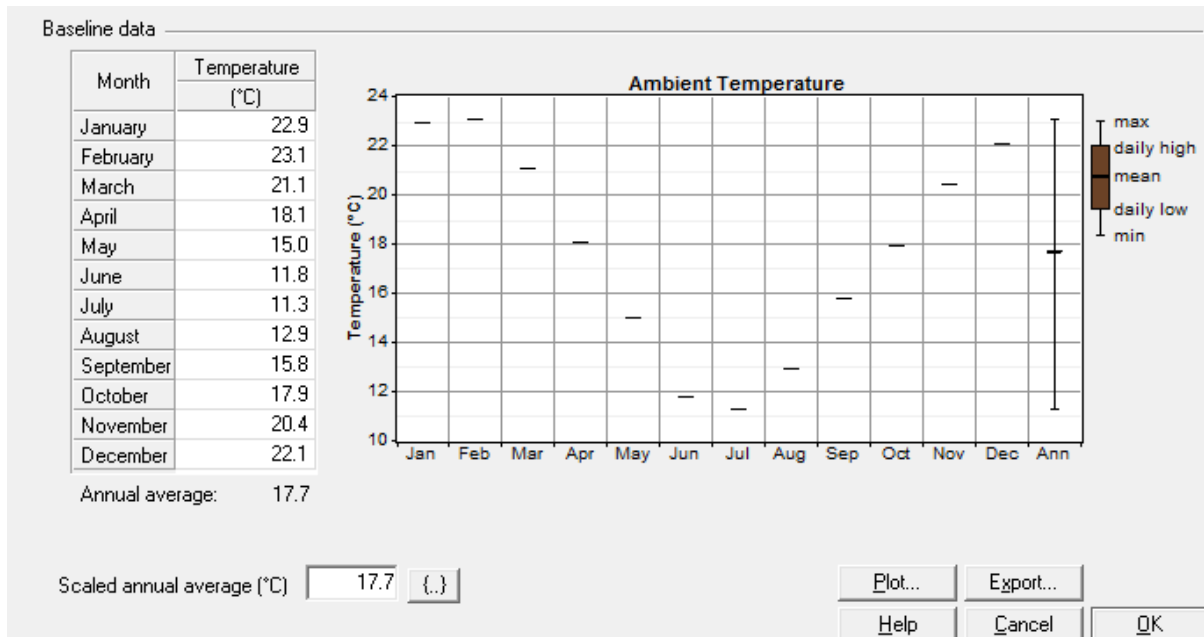


Figure 2. Average monthly air temperatures at the Forrest station.

4.2. System specifications and assumptions

The basic components of the simulated power system was based on the technical specification data of the commercially available “Nomad 27” and “Sherpa 50” manufactured by the company Goal Zero [36]. The “Nomad 27” is a 0.151 m², 1.5 kg monocrystalline PV array rated at 27 W, $V_{SC} \sim 19V$, (buck regulated USB output of 5 V, 0.5 A, 2.5 W max., or a 13–15 V 1.6 A, 24 W max. DC unregulated output), with dimensions of 113 × 57 cm unfolded, able to be folded into a package with dimensions 26.7 × 18 × 5 cm. The simulations included a temperature coefficient of power (%/°C) of -0.269 , a nominal cell operating temperature of 46 °C, and PV derating of 90%, and ground reflectance of 15%. The temperature dependent simulations utilised the average monthly temperature data for the location (Figure 2). The “Sherpa 50” is a 0.50 kg Li-ion (nickel manganese cobalt oxide, NMC) 9–13 VDC battery-charger unit, with dimensions 11.4 × 3.8 × 12.7 cm, and a capacity of around ~56 Wh, comprising of six 3.6 V, 2.6 Ah cells) with a 10 A fuse. The unit is designed to be charged by either the “Nomad” PV range by Goal Zero, an AC wall adapter, or a 12 VDC system. The charging port can utilise 15–25 V DC (30 W max.) chargers, and has a USB port output (able to provide a regulated 5 V 0–1.5 A (7 W max), a regulated 12 V output (0–6 A, 75 W max.), and a sidecar port (9–13 V, 0–10 A, 75 W max.) for use with a purpose-built modified sine wave inverter (110 VAC, 75 W max.) or for coupling with another “Sherpa 50”, and a laptop port providing a regulated 19 VDC (0–5 A, 75 W max.). The simulations assumed a 75% round trip efficiency from charging and discharging the battery bank, and the control regime stipulated a minimum of 30% bank state of charge at all times to enhance battery longevity. To prevent additional battery wear and tear from current spikes during motor startup the Li-ion battery is able to deliver around five-times the current required by the micropump.

The commercial micropump specification data used in the simulation is the KNF NF2.35(XT) micropump [37]. The NF2.35 is a self-priming diaphragm micropump with a motor able to endure

dry pumping and be mounted in any position, with the total micropumping system weighing only 0.2 kg. The pump motor is an electronically commutated brushless DC motor, with a selected voltage of 12 V, rated at 10 W, with a maximum current of 1.0 A. The NF2.35(XT) pump materials in contact with the water include: a robust polyether ether ketone (PEEK) head, a perfluoro-elastomer (FFKM) head and o-rings for corrosive chemical and high temperature resistance, and a polytetrafluoroethylene (PTFE, of teflon) coated diaphragm and a PTFE resonating diaphragm. The micropump system is able to produce a maximum of 1.6 MPa at a flow rate of 100 mL min⁻¹, or 6 L hr⁻¹, of water at 20 °C, with a maximum suction height of 3 m at full rated output. The system assumed the inclusion of a basic pre-filter for macro particulates on the micropump input with zero impact to the pump suction. The technical simulations simplistically assume a zero derating of all system components and output over a one year interval, and discounts any impact of system fouling, maintenance downtime, and assumes a daily average horizontal PV tracking (manual adjustment) to the solar altitude, and zero PV shading. The characteristics of the single primary load (the micropump) are presented in Figure 3. The primary load simulations variability of “day-to-day” and “time-step-to-time-step” were allocated 10% and 5%, respectively to reflect the relatively constant load arbitrarily selected to operate at 10 hours each day for the entire year. The 10 minute simulated time-step variations generated a maximum peak load on a 10 minute basis of around 0.014 kW, consistent with the manufacturer specifications and incorporating expected variability and losses.

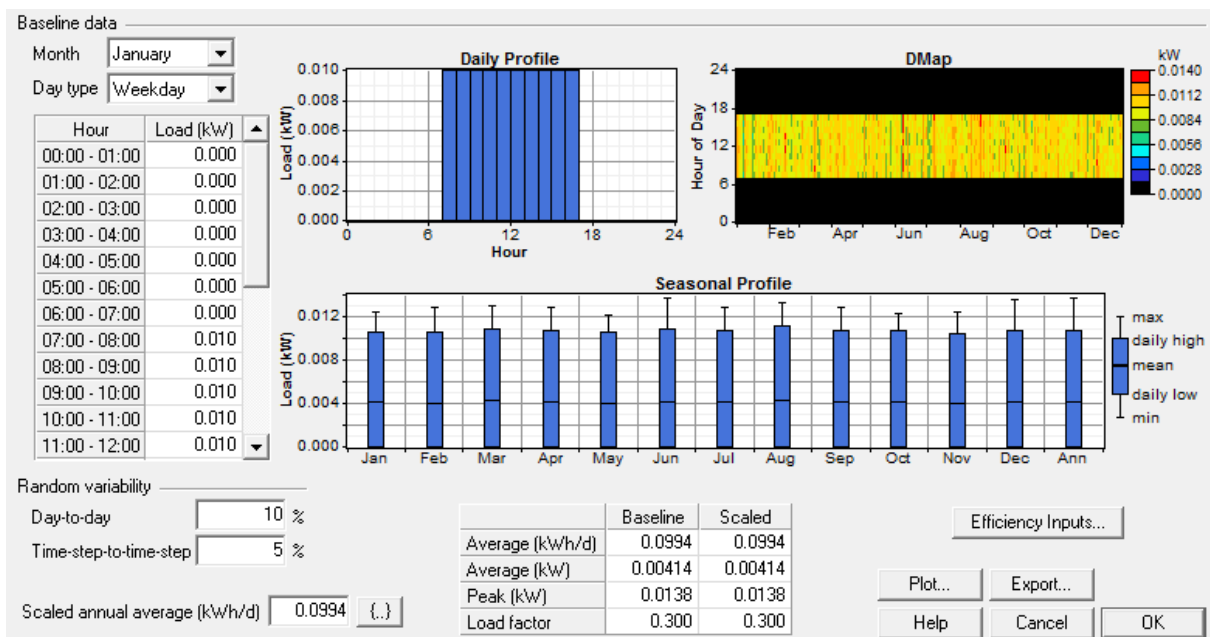


Figure 3. Generated load profile for the remote desalination system.

4.3. Desalination membrane specifications and assumptions

The membrane flux and salt rejection assumptions used in Table 1 are derived from peer-reviewed journal articles described in section 3. The authors wish to clarify that the published flux and salt rejection rates are likely to be overstated in the construction of actual membrane units, as some of published performance data are based on theoretical modelling, sometimes without the material having been produced at scale (or at all in some cases). However, they are suitable

analogies for each technology type for future efficiencies for membrane engineers to approach. The major desalination assumptions include: approximate seawater concentrations (~35,000 ppm TDS), stable water temperatures at 20 °C, a constant pump output at maximum performance (1.6 MPa at a flow rate of 100 mL min⁻¹, or 6 L hr⁻¹, of water at 20 °C), a consistent inlet suction height (of less than 3 m dynamic head), and annual and monthly mean production rate from the PV-battery unit. The assumptions used in the membrane performance calculations include single pass desalination, a 70% water rejection rate, a functional 3 cm² membrane, zero energy recovery, a constant salt rejection rate, system 100% functionality, 10 hours per day manual switching operation, and zero membrane derating over the entire year. Many of these assumptions are arbitrary or unrealistic, especially zero membrane performance derating and fouling, although provide a consistent comparative basis for the potential of each membrane technology type operating at optimal conditions. The 70% water rejection rate was included to maintain the salinities of the feedwater nearer to the initial salinities around the intake from the salt lake, creek, or comparable water body. The very small functional membrane area (3 cm²) is a very conservative assumption, as many membrane technologies of suitable size and weight will be able to be geometrically arranged to achieve much larger functional areas.

Table 1. Peer-reviewed desalination membrane technology performance used for comparison.

RO membrane technology	Reference(s)	Water flux (L cm ⁻² d ⁻¹ MPa ⁻¹)	Salt rejection
Generic quality polymeric	[20,22]	~0.01–0.05	~97–99%
Carbon nanotube polymeric	[20]	0.044	97.7%
Generic polyamide nanofilter	[38–40]	~0.01–0.1	~85–99%
GO polysulphone	[31,32]	~0.19–0.66	10–70%
Graphene	[29,30]	~10–100	“Near 100%”
γ-graphyne-4	[27]	~13	“Perfect rejection”

5. Results

Figures 4 and 5 demonstrate the ability of the selected PV array and Li-ion battery to supply sufficient electricity to the micropump to operate for 10 hours per day at the full rated micropump output for the vast majority (96.6%) of the year, with around 12 hours of pumping demand unmet annually (the equivalent of 1.22 kWh). The battery state of charge is clearly lower in the months from April to September due to lower solar irradiance conditions. The unmet electrical load generally occurs during these intervals, with the simulation generating low irradiance conditions for certain days where the 10 hour operational profile is more difficult to meet. However, as can be seen from Figure 2, the ambient temperatures (and therefore personal water demand) are generally considerably lower than the annual average during this interval. Figure 6 shows a selected screenshot to demonstrate the operational profile of the system over an arbitrary three-day interval.

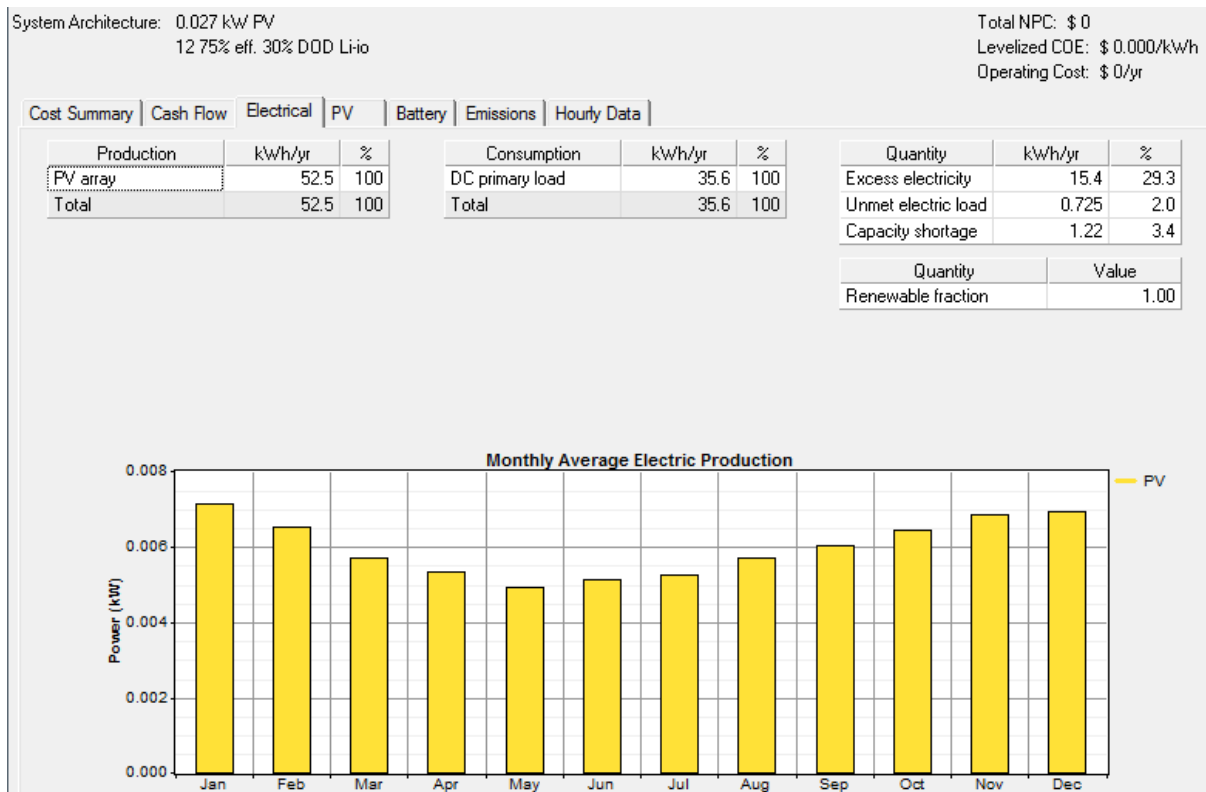


Figure 4. PV monthly generation results of simulations in HOMER.

Table 2 shows the assumed water production based on the micropump specifications and the monthly average output results. Table 2 also includes the daily average minimum performing day percentage total demand shortage; “worst day shortage (%)”, the monthly mean performance of the PV array, the battery bank state of charge, and the resulting assumed micropump water delivery based on the manufacturer specifications. Table 2 clearly shows that the system is able to provide very close to 60 L d⁻¹ for the vast majority of days in the year.

Table 2. Monthly and annual average PV-Li-ion battery-micropump system performance.

Mean daily output/values*	J	F	M	A	M	J	J	A	S	O	N	D	Av.
Global irradiance (W m ⁻²)	320	270	230	180	140	130	140	170	220	260	300	310	220
PV output (Wh d ⁻¹)	173	158	136	130	118	122	127	137	146	156	163	165	144
Battery state of charge (%)	95	94	82	83	73	74	80	82	81	93	91	92	85
Capacity shortage (%)	0	0	3.5	0.15	4.0	4.0	1.2	3.0	2.5	0	0	0	1.4
Worst day shortage (%)	0	0	14	8	24	22	10	12	14	0	0	0	8.5
Micropump (L d ⁻¹)	60	60	57.9	59.1	57.6	57.6	59.3	58.2	58.5	60	60	60	59.16
Min. day micropump (L d ⁻¹)	60	60	51.6	55.2	45.6	46.8	54	52.8	51.6	60	60	60	54.9

*Will not sum due to rounding.

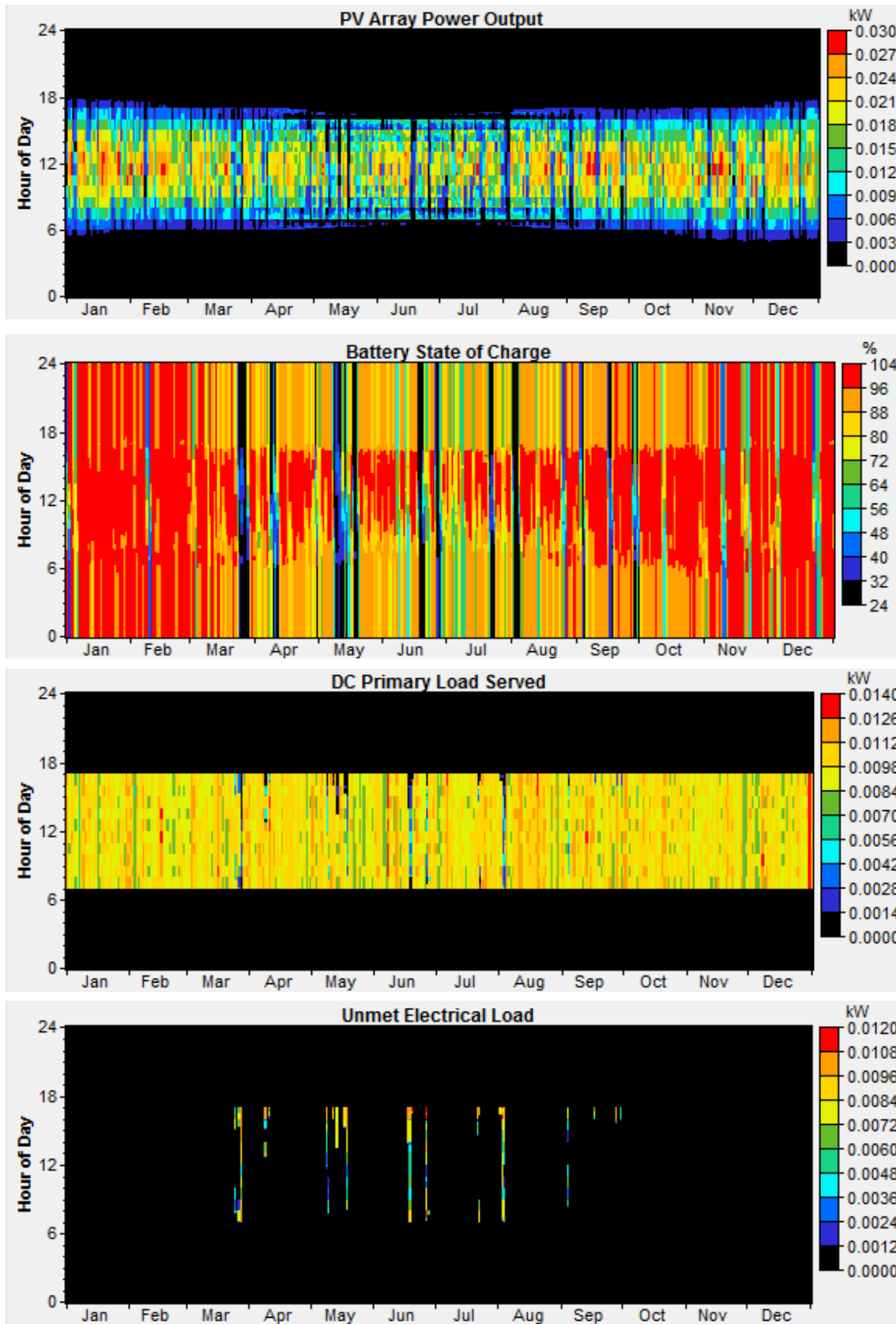


Figure 5. PV generation results of simulations in HOMER.

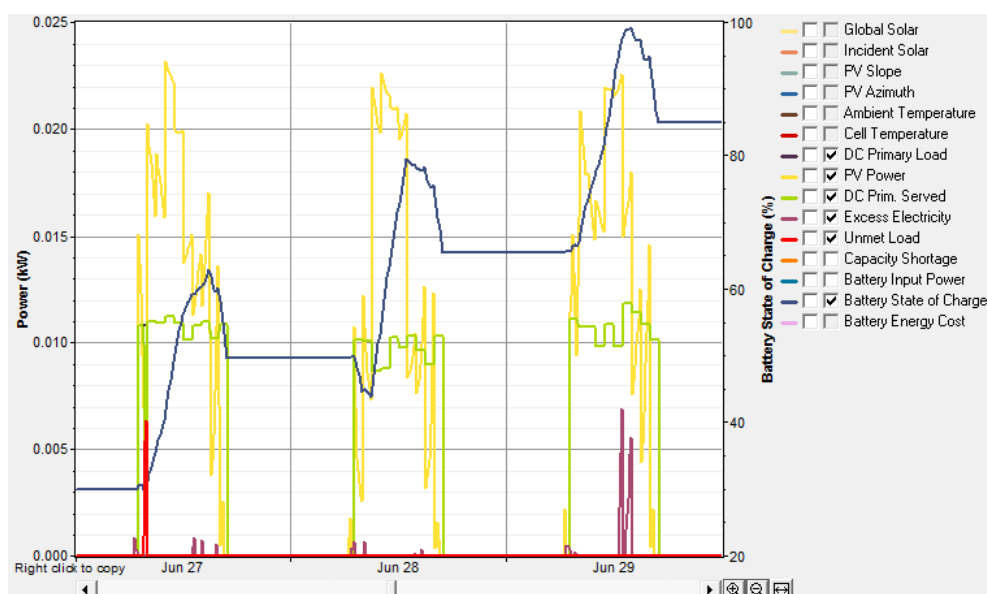


Figure 6. Example screenshot of detailed simulation intervals in HOMER.

Table 3. Assumed freshwater production based on peer-reviewed data and simulations.

RO membrane technology	Water flux ($\text{L cm}^{-2} \text{ h}^{-1} \text{ MPa}^{-1}$)	Drinking water (L d^{-1})*	Salt rejection	Salinity (ppm TDS)*
Generic quality polymeric	~0–0.002	~0–0.288	~97–99%	~1050–350
Carbon nanotube polymeric	~0	~0	97.7%	~805
Generic polyamide	~0–0.004	~0–0.057	~85–99%	~5250–350
GO polysulphone	~0.008–0.0275	~0.11–0.40	~10–70%	~31,500– 10,500
Graphene	~0.416–4.16	~5.9–18**	“Near 100%”	~0
γ -graphyne-4	~0.54	~7.77	“Perfect rejection”	0

*Will not sum due to rounding.

** Note the micropump production of around 60 L d^{-1} is the limiting factor in this theoretical case, and with the assumed 70% rejection of the intake water can in theory only generate 18 L d^{-1} . Otherwise with a larger volume of water under identical conditions the theoretical membrane could produce up to 59.9 L d^{-1} during the 10 hours of operational simulated load per day.

The hourly water flux rate in column 2 of Table 3 (in $\text{L cm}^{-2} \text{ h}^{-1} \text{ MPa}^{-1}$) was calculated by simply dividing the water flux data ($\text{L cm}^{-2} \text{ d}^{-1} \text{ MPa}^{-1}$) in Table 1 by 24 hours. As the micropump is clearly able to provide the vast majority of the water volume at the required pressure necessary for each membrane technology analysed in this research, in general the limiting factor is the membrane flux. The only exception was the very high simulated flux rates of the higher estimates for the graphene membrane. In this case the flow rate of the micropump limited the membrane flux by around 30% of the potential theoretical potential¹. (In practice the rejection rate can be reduced to desalinate additional volumes of water at a declining efficiency.) The resultant drinking water

¹ Example calculation: $0.54 \text{ L cm}^{-2} \text{ h}^{-1} \text{ MPa}^{-1} \times 3 \text{ cm}^2 \times 10 \text{ h} \times 0.3 \times 1.6 \text{ MPa} = 7.77 \text{ L d}^{-1}$.

salinity calculation was a relatively simplistic multiplication of the salt rejection rate as a percentage of the assumed 35,000 ppm TDS feedwater².

The research results show that the first research criterion of utilising only small-scale portable systems suitable for carrying on the person was met by the commercial availability of flexible modules, Li-ion battery-converter units, and high pressure low voltage brushless DC motor-powered micropumps. The total weight of the PV-Li-ion battery-micropump without the membrane unit totalled only 2.2 kg, the equivalent weight of 2.2 L of freshwater. The second research criterion of achieving a minimum fresh water production of 3.5 L day⁻¹ for a portable system was successfully met. The simulation research results demonstrate that commercially available PV-Li-ion battery components would be sufficiently able to supply low voltage brushless DC motors of micropumps to more than able to supply the minimum water needs of an individual producing around 60 L d⁻¹ in a 10 hour daily load cycle. The third criterion of efficiency of design to consume the minimum amount of energy per unit of water, was only made possible through the likely efficiencies of the graphene-based membranes. With the assumed efficiency of the membrane technology performance the simulated system was able to produce between 6 and 18 L d⁻¹ per system, around 2–5 times the target requirement.

The largest sources of system uncertainty in this research are derived from the relatively low data availability of the theoretical membranes, and the robustness of each simulated component under nominal and extreme operating conditions. As such, simulation findings should be used as a guide of future potential as technical performance results will vary depending of the ambient conditions, water quality and temperatures, water head heights, and of future membrane development applications. However, outside of the theoretical performance and simulation considerations, to effectively produce a membrane able to desalinate a wide range of water resources throughout the year with minimal scaling and fouling (or the ability to easily replace a membrane cartridge or maintain the reused membranes), will require much additional research and development. Approaching the theoretical high-efficiency membrane desalination technology treating high TDS saline water and relatively low pressure akin to the theoretical performance expected from graphene-based technologies will be a major challenge. The generic RO polymeric, the generic polyamide, the carbon nanotube polymeric membrane, and the graphene oxide polysulphone water flux and salt rejection data used in this analysis suggested these technologies will be unsuitable for extremely small scale portable systems without large advances in performance. Despite large uncertainties, these technologies are more likely to enhance the performance of existing larger desalination systems, rather than small-scale portable units. The continued development of new generations of graphene-based membranes and the accelerated efforts to manufacture them at commercial scales will be an enlightening phase in desalination technology. There is likely many new possibilities and major revisions in technology performance of various new arrangements, and naturally numerous engineering challenges prior to commercialisation will follow. Nonetheless, the evolution of the “graphene family” and the refinement of potential applications is likely to be an extremely productive field of research, leading to further desalination system improvements and likely a quiet revolution in various applications.

² Example calculation: $(100\% - 99\%) \times 35,000 \text{ ppm TDS} = 350 \text{ ppm TDS}$.

6. Conclusion

The authors recommend further exploration of portable small-scale renewable energy-based and portable desalination systems with lightweight micropump and membrane technologies that exhibit a practical operational robustness for remote areas. The development of suitable, portable, and sustainable desalination systems for remote conditions requires rigorous attention to system designs that enhance reliability and servicing minimisation of commercial systems. There is major need to understand appropriate pre-treatment suitable for such system configurations to reduce the capital, operational, and maintenance costs of maintaining a safe water supply in remote regions that enable mobile individuals to remain healthy and without the fear of lack of drinking water. This research demonstrates that commercially available PV-battery-micropump systems and new generations of energy-efficient membranes under development have the technical future potential to enable users to sustainably procure daily drinking water needs using portable systems that are lower weight than carrying drinking water itself.

Acknowledgements

Sandia National Laboratories is a multi-program laboratory managed and operated by Sandia Corporation, a wholly owned subsidiary of Lockheed Martin Corporation, for the U.S. Department of Energy's National Nuclear Security Administration under contract DE-AC04-94AL85000.

Conflict of Interest

All authors declare no conflict of interests in this paper.

References

1. Belessiotis V, Delyannis E (2001) Water shortage and renewable energies (RE) desalination - possible technological applications. *Desalination* 139: 133–138.
2. Banat F, Jwaied N (2008) Economic evaluation of desalination by small-scale autonomous solar-powered membrane distillation units. *Desalination* 220: 566–573.
3. El-Nasher AM (2001) The economic feasibility of small solar MED seawater desalination plants for remote arid areas. *Desalination* 134: 173–186.
4. Al-Karaghoul A, Renne D, Kazmerski LL (2009) Solar and wind opportunities for water desalination in the Arab regions. *Renew Sust Energ Rev* 13: 2397–2407.
5. Al-Karaghoul A, Renne D, Kazmerski LL (2010) Technical and economic assessment of photovoltaic-driven desalination systems. *Renew Energ* 35: 323–328.
6. Gude VG, Nirmalakhandan N, Deng S (2010) Renewable and sustainable approaches for desalination. *Renew Sust Energ Rev* 14: 2641–2654.
7. Chaibi MT (2000) An overview of solar desalination for domestic and agriculture water needs in remote arid areas. *Desalination* 127: 119–133.
8. Risbey J, Kandlikar M, Dowlatabadi H, et al. (1999) Scale, context, and decision making in agricultural adaptation to climate variability and change. *Mitig Adapt Strat Gl* 4: 137–165.

9. Soric A, Cesaro R, Perez P, et al. (2012) Eausmose project desalination by reverse osmosis and batteryless solar energy: design for a 1 m³ per day delivery. *Desalination* 301: 67–74.
10. De Munari A, Capao DPS, Richards BS, et al. (2009) Application of solar-powered desalination in a remote town in South Australia. *Desalination* 248: 72–82.
11. Banat F, Qiblawey H, Al-Nasser Q (2012) Design and operation of small-scale photovoltaic-driven reverse osmosis (PV-RO) desalination plant for water supply in rural areas. *CWEEE* 1: 31–36.
12. Banasiak LJ, Schafer AI (2009) Removal of inorganic trace contaminants by electrodialysis in a remote Australian community. *Desalination* 248: 48–57.
13. Bennett R (2013) System and method for water purification and desalination. US, Lockheed Martin Corporation, 10.
14. Lazarov V, Zarkov Z, Kanchev H, et al. (2012) Compensation of power fluctuations in PV systems with supercapacitors. *E+E* 47: 48–55.
15. Glavin ME, Hurley WG (2012) Optimisation of a photovoltaic battery ultracapacitor hybrid energy storage system. *Solar Energ* 86: 3009–3020.
16. McHenry MP (2009) Remote area power supply system technologies in Western Australia: New developments in 30 years of slow progress. *Renew Energ* 34: 1348–1353.
17. McHenry MP (2009) Why are remote Western Australians installing renewable energy technologies in stand-alone power supply systems? *Renew Energ* 34: 1252–1256.
18. Architectural Energy Corporation (1991) Maintenance and operation of stand-alone photovoltaic systems. Albuquerque, New Mexico, and Boulder, Colorado, USA: Sandia National Laboratories.
19. Anand S, Fernandes BG (2010) Optimal voltage level for DC microgrids. 36th Annual Conference on IEEE Industrial Electronics Society (IECON), Glendale, Arizona, USA.
20. Lee KP, Arnot TC, Mattia D (2011) A review of reverse osmosis membrane materials for desalination - Development to date and future potential. *J Membrane Sci* 370: 1–22.
21. Hassan AF, Fath HES (2013) Review and assessment of the newly developed MD for desalination processes. *Desalin Water Treat* 51: 574–585.
22. Wang EN, Karnik R (2012) Water desalination: Graphene cleans up water. *Nat Nanotechnol* 7: 552–554.
23. Ahmadun F-R, Pendashteh A, Abdullah LC, et al. (2009) Review of technologies for oil and gas produced water treatment. *J Hazard Mater* 170: 530–551.
24. Guillén-Burrieza E, Zaragoza G, Miralles-Cuevas S, et al. (2012) Experimental evaluation of two pilot-scale membrane distillation modules used for solar desalination. *J Membrane Sci* 409–410: 264–275.
25. Guillén-Burrieza E, Blanco J, Zaragoza G, et al. (2011) Experimental analysis of an air gap membrane distillation solar desalination pilot system. *J Membrane Sci* 397: 386–396.
26. Onsekizoglu P (2012) Membrane distillation: principle, advances, limitations and future prospects in food industry. In: Zereshki S, Ed. *Distillation - advances from modeling to applications*. Rijeka, Croatia, InTech, 233–266.
27. Zhu C, Li H, Zeng XC, et al. (2013) Ideal desalination through graphyne-4 membrane: nanopores for quantized water transport. *Condensed Matter* arXiv: 1307.0208
28. Tang Q, Zhou Z, Chen Z (2013) Graphene-related nanomaterials: tuning properties by functionalization. *Nanoscale* 5: 4541–4583.

29. Cohen-Tanugi D, Grossman JC (2012) Water Desalination across Nanoporous Graphene. *Nano Letters* 12: 3602–3608.
30. Cohen-Tanugi D (2012) Nanoporous graphene as a desalination membrane: a computational study. Department of Materials Science and Engineering, Cambridge, Massachusetts, USA, Massachusetts Institute of Technology.
31. Ganesh BM, Isloor AM, Ismail AF (2013) Enhanced hydrophilicity and salt rejection study of graphene oxide-polysulfone mixed matrix membrane. *Desalination* 313: 199–207.
32. Hu M, Mi B (2013) Enabling graphene oxide nanosheets as water separation membranes. *Environ Sci Technol* 47: 3715–3723.
33. Cranford SW, Buehler MJ (2011) Mechanical properties of graphyne. *Carbon* 49: 4111–4121.
34. Zheng JJ, Zhao X, Zhao Y, et al. (2013) Two-dimensional carbon compounds derived from graphyne with chemical properties superior to those of graphene. *Sci Rep* 3: 1271.
35. Department of Natural Resources Canada. RETScreen Version 4. (2010) Available from: <http://www.nrcan.gc.ca/energy/software-tools/7465>.
36. Goal Zero (2013) Available from: <http://www.goalzero.com/>.
37. KNF (2013) Diaphragm liquid pump data sheet NF 2.35. Available from: <http://www.knfusa.com/pdfs/nf2-35.pdf>.
38. Amouha MA, Gholam RNB, Behnam H (2011) Nanofiltration efficiency in nitrate removal from groundwater: a semi-industrial case study. International Conference on Environmental Engineering and Applications (ICEEA), Shanghai, China.
39. The Dow Chemical Company (2013) Dow Filmtec™ NF90 nanofiltration elements for commercial systems. Available from: http://www.dowwaterandprocess.com/en/products/f/filmtec-nf90_4040.
40. Xie W, Geise GM, Freeman BD, et al. (2012) Polyamide interfacial composite membranes prepared from m-phenylene diamine, trimesoyl chloride and a new disulfonated diamine. *J Membrane Sci* 403–404: 152–161.



AIMS Press

© 2016 Mark P. McHenry, et al., licensee AIMS Press. This is an open access article distributed under the terms of the Creative Commons Attribution License (<http://creativecommons.org/licenses/by/4.0>)